Computers and Electronics in Agriculture 154 (2018) 341–346

Contents lists available at ScienceDirect

Computers and Electronics in Agriculture

journal homepage: www.elsevier.com/locate/compag

Original papers

A computer vision approach based on endocarp features for the identification of olive cultivars

S. Satorres Martínez[a,*], D. Martínez Gila[a], A. Beyaz[b], J. Gómez Ortega[a], J. Gámez García[a]

[a] System Engineering and Automation Department, University of Jaén, Jaén 23071 Spain
[b] Department of Agricultural Machinery and Technologies Engineering, Faculty of Agriculture, Ankara University, Ankara, Turkey

ARTICLE INFO

Keywords:
Endocarp features
Computer vision
Olive varietal identification
Wilk's Lambda
Partial least squares discriminant analysis

2010 MSC:
00-01
99-00

ABSTRACT

The identification of olive cultivars is of utmost importance for a multitude of factors affecting both, the olive oil elaboration process and fair trade exchanges. The accurate varietal identification is a time consuming task that requires trained specialists or expensive and specific equipment. When applying the traditional method, a specialist assesses morphological features using the olive endocarp. A proposal to automate this identification method is presented in this paper. Endocarp images, acquired under three different perspectives, are processed to extract the same information that the specialist utilizes. Then, the partial least squares discriminant analysis classifier, with or without feature selection, has been tested on a set of 250 samples from 5 different varieties. Results show that the proposal is an alternative identification method which could also be used in the traditional one in order to assist the specialist in the determination of the variety.

1. Introduction

The accurate identification of olive cultivars is now a necessity for companies from the olive oil sector. To produce olive oil Protected by a Designation of Origin (PDO), the traceability of the fruits as well as the confirmation of their geographical origin and authenticity is a must (Likudis, 2016). The POD labelling constitutes a great motivation for a wide range of consumers, as it is considered to be associated with high-quality products, and in fact it is (Parra-López et al., 2015). Having a precise knowledge of the raw materials, fruits varieties in this case, allows a better adjustment of the parameters involved in the olive oil productive process, which is related to the final product quality and yield (Ram et al., 2010).

Nowadays, two different methods are utilized to determine the varietal origin: genetic and morphological ones (Trujillo et al., 2014b). The genetic method is more accurate but require a special equipment used by experts with specialist knowledge only. The morphological one focuses on the analysis of the olive tree, flowers, leaves, fruits and endocarps (the outer part of the olive stones) (Blazakis et al., 2017). Although features extracted from the former sources are assessed within this method, the endocarp information is the most valuable. This is because the olive stone is less dependent of environmental conditions, therefore, features extracted from this source are quite similar for olives belonging to the same variety, and distinct for different ones.

Thus, the morphological method is most often used because of its cost, efficiency and repeatability (Laaribi et al., 2017), even though being a manual process subjected to human errors. The use of technology to facilitate the specialist work, or even the fully automation of the method, would be a valuable contribution.

A technology with a considerable potential for agriculture industry is computer vision (Sun, 2016). Because of low cost, rapid inspection rate, and the ability to provide accurate and consistent information, this technology has been applied in a plethora of applications. A comprehensive review in quality inspection of fruit and vegetables using computer vision can be found in Zhang et al. (2014). Traditional computer vision systems and also the latest developments using hyperspectral and multispectral systems were also reported in this paper. Quality inspection of olive fruits, processing infrared images, was developed in Guzmán et al. (2013). In recent works, the maturity of the fruits was estimated by following the evolution of the colour in the maturity process (Avila et al., 2015) or following the evolution of the electrical conductivity in the mesocarp (Justicia et al., 2017).

The identification of olive varieties, by computer vision, has been and continues to be an active research area. Diaz (2016) classified processed olives into four categories applying a Bayesian discriminant analysis. Bari et al. (2003) characterized nine olive genotypes using fractals in combination with moments and statistical classifiers. Beyaz et al. studies (Beyaz and Öztürk, 2016; Beyaz et al., 2017) concentrated

* Corresponding author.
E-mail address: satorres@ujaen.es (S. Satorres Martínez).

https://doi.org/10.1016/j.compag.2018.09.017
Received 15 May 2018; Received in revised form 7 September 2018; Accepted 14 September 2018
Available online 20 September 2018
0168-1699/

on identifying Turkish and Spanish cultivars extracting features from fruits, leaves and stones. Piras et al. (2016) studied the use of endocarps biometric features for determining relationships between wild and framed olives. Vanloot et al. (2014) classified the five main French cultivars with a hit rate of 100 percent.

The purpose of this paper is to develop a procedure with two main functionalities. The first one is to assist the specialist in the work-intensive task of the morphological method application. By making use of computer vision to extract the endocarp features, detailed in the official method, the specialist could use this information to make his work less laborious. The second one is give an approach for the fully automation of the traditional morphological method that makes use of the endocarp features for varieties identification.

The remainder of this paper is organized as follows. Section 2 presents the varieties used for this analysis and the preparation method for obtaining the olive endocarps. In addition, the image acquisition set-up and image processing algorithms are also detailed. Section 3 shows the experimental validation of the method and a comparative study of the different classifiers developed for variety identification. Finally, the conclusions are drawn in Section 4.

2. Material and methods

The proposed procedure to identify varieties considers two different stages, five main steps and two functionalities (Fig. 1). The design stage is only executed once, with the purpose of modelling the features, analysed by the expert when applying the morphological method (Trujillo et al., 2014a), and designing the classifier. Then, in the operating stage, the images acquired are processed to provide the application functionalities. Through the first functionality the endocarp features are given to the specialist and within the second one endocarp olives are automatically classified. In the next subsections the main stages of the procedure are deeply detailed.

2.1. Step 1. Olive samples and endocarp preparation

Fruits from 5 varieties of framed olives, with varietal certification, were collected during Jan-Feb 2018 from different olives orchards located in Andalusia, a region in the south of Spain. The olives were manually collected when the fruits reached a maturity index of 5. In this state of ripeness, the fruit skin is completely black and less than half of its flesh is turning purple. At this stage the endocarp is completely developed. To ensure that the samples are representatives, several trees were chosen with a comparable crop load and homogeneous maturity. Then, a total of 250 fruits, 50 per variety, were picked up from around the trees at the middle of their crown. Table 1 shows the list of cultivars, the origin of the samples and the certifying organism.

The harvested olives were processed to obtain the endocarps. For this, three different cleaning methods were applied: water jet machine, ultrasonic cleaner and bleach solution. With the first method, the olive stone was over cleaned and part of its texture was damaged. The second one was not a valid alternative too. In this case, there were remains of biological material in the endocarp texture. Best results were achieved with the last method, the bleach solution. By applying a 5% bleach solution during one hour, there were a complete absence of biological material (brown colour) and no damage appears in the endocarp texture (Fig. 2).

Table 1
Detail of the olive samples collected in Andalusia (Spain).

Cultivar	Area of cultivation	Certifying organism
Picudo	Worldwide varieties collection (Córdoba)	IFAPA, Alameda del Obispo
Lucio	Worldwide varieties collection (Córdoba)	IFAPA, Alameda del Obispo
Cortijuelo	Montefrío (Granada)	In process of certification (CARDIOLIVE project)
Manzanillo	Worldwide varieties collection (Córdoba)	IFAPA, Alameda del Obispo
Negrillo	Worldwide varieties collection (Córdoba)	IFAPA, Alameda del Obispo

2.2. Step 2. Image acquisition

Images were acquired by means of a CMOS camera Genie Nano G3-GC11-C2420 with colour sensor, 2464 × 2056 resolution and 3.45 μm pixel size. The camera, with a lens of 50 mm and extension tubes of 15 mm, was placed at 180 mm from the endocarp.

Every endocarp was placed in three different positions: in face and profile in front of the camera and vertical position parallel to the optical axis of the camera. The field of view was obtained taken into account the most restrictive case: highest dimension in face or profile image. Referring to Eq. (1) the Field Of View, FOV, was calculated as (Hornberg, 2006):

$$FOV = maximum\ endocarp\ size + tolerance\ in\ positioning + margin + adaptation\ to\ aspect\ ratio\ of\ camera\ sensor \quad (1)$$

where the maximum endocarp size was 2.5 mm, the tolerance and margin was 0.5 mm and the aspect ratio was 4:3. Hence, the FOV was calculated as (Eq. (2)):

$$FOV_{vertical} = 2.5\ \text{mm} + 0.5\ \text{mm} + 0.5\ \text{mm} = 3.5\ \text{mm}$$
$$FOV_{horizontal} = 3.5\ \text{mm} \cdot \frac{4}{3} = 4.66\ \text{mm} \quad (2)$$

2.3. Step 3. Image segmentation

The main goal of this step is to separate the endocarp from the background. Fig. 3 shows the image segmentation procedure. First, four images (the three colour channels and the monochrome) are fused into one. In the fused image the contrast between the endocarp and its furrows and the endocarp and the background is maximized. The

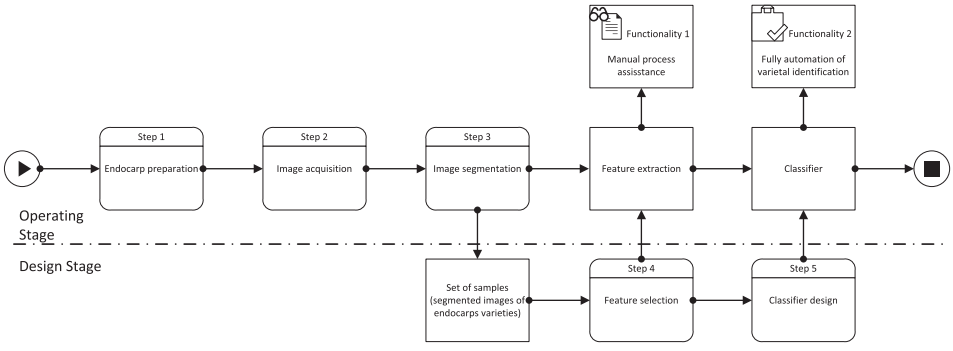

Fig. 1. Overview of the automated procedure for the identification of olives varieties.

Fig. 2. Effect of bleach solution in the endocarp texture.

transformed grey value in the high contrasted image, $t_{r,c}$, only depends on the grey value $g_{r,c}$ in the input image at the same position. Therefore, the transformation is implemented by Eq. (3) as:

$$t_{r,c} = f_g[g_{r,c}] \tag{3}$$

where the [ ] operator denotes the table look-up. Second, a global thresholding technique has been utilized for image segmentation, the Ridler method (Russ, 2011). This method produces satisfactory results with images that present a bimodal o multimodal distribution with an homogeneous background. Ridler is an iterative procedure that finishes when: $|U_{n-1} - U_n| < difference$, $difference$ is a parameter empirically determined. The optimal threshold U_{opt} is obtained from the Eq. (4):

$$U_{opt} = \lim_{n\to\infty} \frac{m_e(T_n) + m_b(T_n)}{2} \tag{4}$$

where T_n is the threshold at iteration n, $m_e(T)$ and $m_b(T)$ are the average grey level values of the endocarp and the background, respectively, defined as (Eq. (5)):

$$m_e(T) = \sum_{g=T+1}^{G} g \cdot p(g)$$
$$m_b(T) = \sum_{g=0}^{T} g \cdot p(g) \tag{5}$$

being $p(g)$ the probability mass function calculated according to the Eq. (6):

$$p(g) = \frac{h(g)}{M} \tag{6}$$

where $h(g)$ is the image histogram and M the number of pixels in the image. Finally, morphological image processing is used to restore the regions corresponding to the endocarp and more specifically closing operation. Denoted by $A \cdot B$ the closing operation is a dilation followed by an erosion (Eq. (7)):

$$A \cdot B = (A \oplus B) \ominus B \tag{7}$$

where B is the structuring element that is defined considering the geometry of the region that should be restored. A disk shaped structuring element has been used in this image processing step.

2.4. Step 4. Feature extraction

A methodology for the identification of olive varieties by endocarp features was published in International Olive Council (2000). In this catalogue the endocarps were characterized by shape, symmetry in two different positions, maximum transversal width, apex, basis, surface, mucro (apex summit) and fibrovascular furrow distribution. This knowledge is utilized by the automated procedure for the identification of olives varieties.

From the endocarps, segmented in the former step, eight set of features have been extracted. The aim was to offer the same type of information handled by the specialist, first functionality of the procedure, and to use it in the second functionality, that is, the fully automation of varietal identification.

Table 2 presents the morphological endocarp features described in International Olive Council (2000) and how they were derived from the image processing algorithms. A total of 46 features were extracted from three different images. Six features to describe shape, symmetry (in two positions), maximum transversal width and apex and base shape (Fig. 4).

For describing the endocarp surface and the fibrovascular distribution, 20 features were analyzed in two images (in face in front of the camera, position A, and vertical position parallel to the optical axis). Measures based on statistical properties of the intensity histogram and the Haralick descriptors were used to describe the texture and are presented in Table 3.

These features are not equally informative among varieties; some of them may be noisy, correlated or irrelevant. Selecting a set of relevant features reduces the volume of computation, measurement and storage requirements, along with other factors, making the classifier more efficient. For feature selection the Wilk's Lambda criterion was used (el Ouardighi et al., 2007). Fig. 5 shows the Wilk's Lambda (λ_j) for each of the 40 texture features. It is important to note that the feature is more discriminative if λ_j is small. Features leading a better discrimination were included in one of the classifiers and it is detailed in the next section.

2.5. Step 5. Classifier design

A supervised classification algorithm, Partial Least Squares Discriminant Analysis (PLS-DA), based on the features extracted in the previous step, has been implemented to classify each olive endocarp sample according to its variety. PLS-DA is a linear classification method that combines the properties of partial least squares regression with the discrimination power of a classification technique (Ballabio and Consonni, 2013). It searches linear combinations of the features, so-called Latent Variables (LVs), in order to maximize the covariance with the classes, the olive varieties in this case. The general underlying model of multivariate PLS-DA appears in the (Eq. (8)):

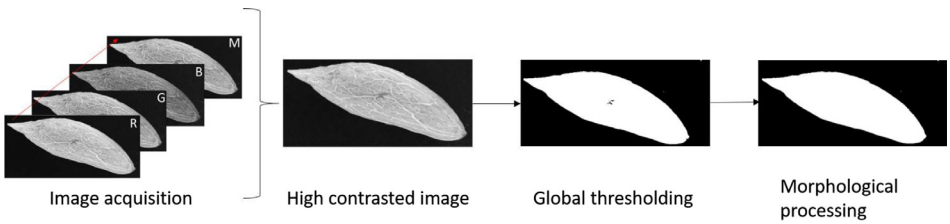

Fig. 3. Image segmentation procedure.

Table 2
List of the most representative endocarp features.

Feature	Description	Implementation
Shape	Determined by the endocarp length and width (spherical, ovoidal, elliptical and elongated)	Length and Width ratio (L/W) of the endocarp bounding box
Symmetry (Position A)	Determined by the correspondence between the two longitudinal halves in face position (symmetric, sightly symmetric, asymmetric)	Segmented images Overlap in percentage (%O)
Symmetry (Position B)	Determined by the correspondence between the two longitudinal halves in profile position (symmetric, slightly symmetric)	Segmented images Overlap in percentage (%O)
Maximum transversal width	Distance from the endocarp base or apex to its maximum transverse diameter (towards the base, centered, towards the apex)	Distance from the apex to the endocarp minor axis
Apex	Assessed by the apex shape (pointed, rounded)	Apex angle
Base	Assessed by the base shape (pointed, truncated, rounded)	Base angle
Surface	Assessed by the endocarp texture (smooth, rough, scabrous)	Surface texture measured by Haralick (14 features) and statistical measures (6 features)
Fibrovascular furrow distribution	Assessed by the furrow distribution placing the endocarp in a vertical position (uniform, grouped close to the suture)	Furrow texture measured by Haralick (14 features) and statistical measures (6 features)

$$X = TP^T \tag{8}$$

$$Y = UQ^T$$
$$U = T\beta$$

where T represents the scores of X, P is the matrix with the loadings of X, U contains the scores of Y, Q is the matrix of loadings of Y. Loadings can be interpreted as the weights of each feature to determine the LVs, while scores represent the coordinates of samples in the LV projection hyperspace. Furthermore, β contains the regression coefficients which provide the relationship between U and T. Substituting the resulting model can be expressed as Eq. (9) shows.

$$Y = UQ^T = T\beta Q^T = XP\beta Q^T \tag{9}$$

$$\widetilde{B} = P\beta Q^T$$

According to the $\widetilde{B}$ coefficients, PLS-DA returns estimated values ($\hat{y}_i$) for each i_{th} sample (Eq. (10)). So, the probability of belonging to a specific class g_{th} can be obtained through the probability density function of each class (Eq. (11)).

$$\hat{y}_i = x_i^T \widetilde{B} \tag{10}$$

$$p(\hat{y}_i|g) = \frac{1}{N}\sum_{n=1}^{N} g_n(\hat{y}_i) \tag{11}$$

where N is the number of calibration samples for the g class and $g_n(\hat{y}_i)$ is the potential function over each PLS prediction (Pérez et al., 2009). In this way, low values of $p(\hat{y}_i|g)$ means that the i_{th} sample does not likely belong to the g_{th} class, otherwise high values closer to one would indicate the opposite. Therefore, the classification issue is carried out by choosing, among all the classes, the one that has the highest probability. Under this approach, the samples are always classified in one of the classes.

The optimal number of texture features was selected according to the minimum error in leave one out cross-validation. It is an iterative process where the number of iterations is equal to the number of samples s. For each iteration the algorithm employs the s_{th} for testing and the rest of samples for training the model. Fig. 6 presents the results when PLS-DA was performed to select the optimal number of texture features and it denotes that the minimum percentage of error (11%) was reached with 19 features. Therefore, the most discriminant features considered in the $PLSDA_{M\&Wilks}$ classifier were the 6 morphological features and the first 19 texture features whose identifiers are presented in the x-axis, Fig. 5. The correspondence between the features identifiers (IDs) and their description is shown in Table 3.

Table 3
List of 20 texture features measured in two images and calculated according to Russ (2011), Gonzalez and Woods (2017).

Features IDs	Feature description
1, 21	Angular Second Moment (Energy)
2, 22	Contrast
3, 23	Correlation
4, 24	Variance
5, 25	Inverse Difference Moment (Homogeneity)
6, 26	Sum Average
7, 27	Sum Variance
8, 28	Sum Entropy
9, 29	Entropy
10, 30	Difference Variance
11, 31	Difference Entropy
12, 32	Information Measure of Correlation I
13, 33	Information Measure of Correlation II
14, 34	Maximal Correlation Coefficient
15–17, 35–37	Average Intensity RGB
18–20, 38–40	Average Intensity HSV

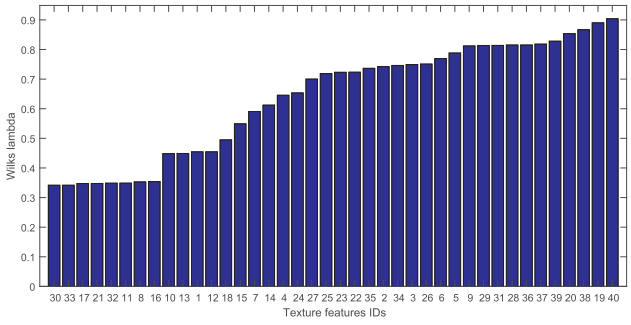

Fig. 5. Wilk's Lambda evolution for texture features.

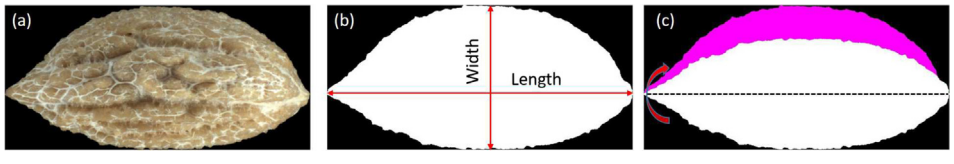

Fig. 4. Feature extraction. (a) Original image; (b) segmented image with endocarp width and length; (c) symmetry in A position (magenta colour indicates the non-overlapped area after the lower part of the image projection). (For interpretation of the references to color in this figure legend, the reader is referred to the web version of this article.)

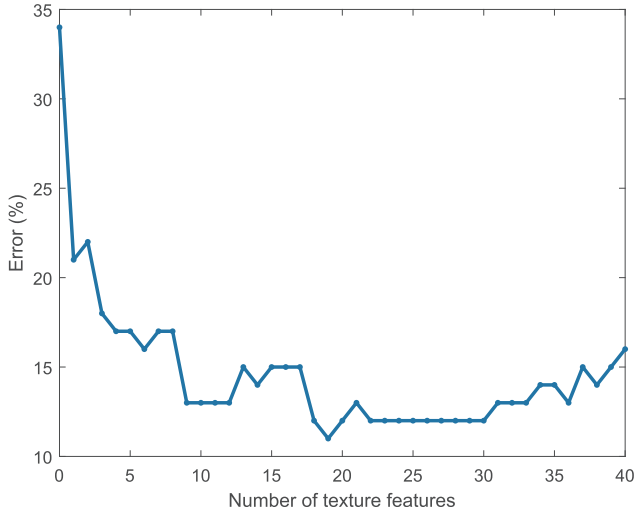

Fig. 6. Calculation of the optimal number of texture features.

3. Results and discussion

A total of 250 samples for five Andalusia varieties—Picudo, Lucio, Cortijuelo, Manzanillo de Montefrio, Negrillo de Estepa—were utilized to assess the proposal. A simple visual examination of the endocarps was sufficient to comprehend the difficulty of the problem. Some of these varieties were similar in shape and was not possible to see significant differences in texture. Table 4 shows the maximum, minimum and average value for the first six features, those which describe shape, symmetry (S_{posA}, S_{posB}), maximum transversal width (MTW), apex and base shape.

As can be seen from these values, some features were not enough discriminative between classes causing a potential damage in the classifier performance. Despite this, geometrical features are given because they integrate the information handled by the specialist when the morphological method is applied. The influence of incorporating texture features has also been analysed. Table 5 shows the classification results considering only the 6 morphological features ($PLSDA_M$), the 46 features ($PLSDA_{all}$) and morphological and the 19 most discriminative texture features computed by Wilk's ($PLSDA_{M\&Wilks}$). These results were reached with hold out validation 80%−20% and they present the average accuracy and error over 1000 iterations. Samples well and wrongly classified are assessed through the following parameters: precision (Pr_g), sensitivity (Sn_g), specificity (Sp_g), accuracy (AC) and error (ER).

Table 4
Shape features values for the different varieties.

Features		Varieties				
		Picudo	Lucio	Cortijuelo	Manzanillo	Negrillo
Shape	Max	2.10	2.07	2.04	1.63	1.67
	Min	1.49	1.68	1.43	1.27	1.25
	Av.	1.71	1.83	1.70	1.44	1.46
S_{posA}	Max	92.32	96.58	99.58	97.91	97.28
	Min	69.60	75.56	56.18	73.28	74.10
	Av.	81.22	89.55	79.53	89.62	87.82
S_{posB}	Max	98.37	97.86	98.58	99.52	99.40
	Min	77.24	79.27	78.29	71.67	87.26
	Av.	91.18	87.75	91.82	86.23	94.03
MTW	Max	59.34	53.81	52.15	54.01	60.00
	Min	51.27	39.00	35.65	34.48	43.51
	Av.	55.40	44.47	43.04	46.98	49.59
Apex	Max	102.82	71.81	75.44	88.54	88.62
	Min	71.19	56.57	46.66	45.92	51.71
	Av.	85.65	64.36	63.18	62.48	70.61
Base	Max	73.35	81.44	74.24	63.16	66.26
	Min	51.94	62.29	51.71	48.79	42.22
	Av.	62.10	71.43	63.32	55.41	57.38

Table 5
Varieties identification.

Classifier	Class	Precision	Sensitivity	Specificity	Accuracy	Error
$PLSDA_M$	Picudo	0.66	0.94	0.88	66%	34%
	Lucio	0.82	0.84	0.95		
	Cotijuelo	0.67	0.53	0.94		
	Manzanillo	0.60	0.51	0.91		
	Negrillo	0.53	0.49	0.89		
$PLSDA_{all}$	Picudo	0.86	0.93	0.96	84%	16%
	Lucio	0.87	0.87	0.97		
	Cotijuelo	0.87	0.86	0.97		
	Manzanillo	0.78	0.71	0.95		
	Negrillo	0.83	0.85	0.96		
$PLSDA_{M\&W}$	Picudo	0.85	0.97	0.96	89%	11%
	Lucio	0.97	0.87	0.99		
	Cotijuelo	0.86	0.91	0.96		
	Manzanillo	0.86	0.77	0.97		
	Negrillo	0.90	0.91	0.97		

(Pr_g) is the ratio between samples correctly classified and the total number of samples correctly and incorrectly assigned for each class (Eq. (12)); (Sn_g) presents the ratio between samples correctly classified and the total number of samples belonging to each class (Eq. (13)); (Sp_g) denotes the ability to reject samples of all the other classes (Eq. (14)); and (AC) is the percentage of correctly classified samples (Eq. (15)).

$$Pr_g = \frac{n_{gg}}{n'_g} \tag{12}$$

$$Sn_g = \frac{n_{gg}}{n_g} \tag{13}$$

$$Sp_g = \frac{\sum_{k=1}^{G}(n'_k - n_{gk})}{n - n_g} \text{ for } k \neq g \tag{14}$$

$$AC = \frac{\sum_{g=1}^{G} n_{gg}}{n} \tag{15}$$

where n'_g is the total number of samples assigned to the g-th class, n_{gg} is the number of samples belonging to class g and correctly assigned to class g, n_{gk} is the number of samples belonging to class g and incorrectly assigned to class k, n_g is the total number of samples belonging to the g-th class, n'_k is the total number of samples assigned to the k-th class (Eq. (16)), n is the total number of samples and G is the total number of groups.

$$n'_k = \sum_{g=1}^{G} n_{gk} \tag{16}$$

As would be expected worst classification rates were obtained using PLSDA only with morphological features, reaching an average accuracy of 66%. By including texture features the results showed a significant improvement (average accuracy 84%). Note that for some varieties the texture information is crucial. In the Negrillo variety the correct classification rate shows an improvement of 30% for $PLSDA_{all}$ or 37% for $PLSDA_{M\&Wilks}$.

Best results were obtained including morphological and the most discriminative features in the PLSDA classifier. The average accuracy for the assessed samples was 89%. This classifier yields good results for all the varieties ranging from 85% (Picudo) to 97% (Lucio). In most of the cases the precision was improved with the $PLSDA_{M\&Wilks}$ classifier,

except for Picudo and Cortijuelo which presented a slight worsening. However, the improvement in precision for the rest of the varieties justify the necessity of feature selection.

4. Conclusion

The varietal identification for olives is an issue of critical importance in the olive oil sector. Traditional methods are mostly based on the visual analysis of the olive endocarp, known as morphological, or those one that require special equipment, genetic methods. In this work we have proposed a system based on computer vision with two main functionalities. The first one is to assist the specialist when applying the morphological method. Morphological features such as shape, symmetry, maximum transversal width, apex, and basis are measured by computer vision. The second is to identify olive varieties utilizing endocarp features. In order to fulfil this task, a supervised classification algorithm, Partial Least Square Discriminant Analysis (PLSDA), was implemented. The effect of including texture features and also the most discriminative texture features was also studied. The best result in the identification of 5 olive Spanish varieties was achieved using the PLSDA classifier with a selection of the most discriminant texture features implemented by Wilk's. Other potential application of this proposal could be its use in an oil mill.

Acknowledgement

This work has been partially supported by the project DPI2016-78290-R. The authors thank the worldwide varieties collection IFAPA and the CARDIOLIVE project (ITC-20151142) for the olive samples provided to carry out this study.

Appendix A. Supplementary material

Supplementary data associated with this article can be found, in the online version, at https://doi.org/10.1016/j.compag.2018.09.017.

References

Avila, F., Mora, M., Oyarce, M., Zuñiga, A., Fredes, C., 2015. A method to construct fruit maturity color scales based on support machines for regression: application to olives and grape seeds. J. Food Eng. 162, 9–17.

Ballabio, D., Consonni, V., 2013. Classification tools in chemistry. Part 1: linear models. PLS-DA. Anal. Methods 5, 3790.

Bari, A., Martin, A., Boulouha, A., Gonzalez Andujar, J.L., 2003. Characterization and identification of olive genotypes using an image feature extraction approach. In: IX Conferencia Espanola de Biometria La Coruna, 2003, pp. 5–8.

Beyaz, A., Öztürk, R., 2016. Identification of olive cultivars using image processing techniques. Turk. J. Agric. For. 40, 671–683.

Beyaz, A., Özkaya, M.T., çen, D., 2017. Identification of some spanish olive cultivars using image processing techniques. Sci. Hortic. 225, 286–292.

Blazakis, K.N., Kosma, M., Kostelenos, G., Baldoni, L., Bufacchi, M., Kalaitzis, P., 2017. Description of olive morphological parameters by using open access software. Plant Methods 13, 111.

Diaz, R., 2016. Classification and quality evaluation of table olives. In: Computer Vision Technology for Food Quality Evaluation. Elsevier, pp. 351–367. https://doi.org/10.1016/B978-0-12-802232-0.00014-1. <http://linkinghub.elsevier.com/retrieve/pii/B9780128022320000141> .

el Ouardighi, A., el Akadi, A., Aboutajdine, D., 2007. Feature selection on supervised classification using Wilks lambda statistic. In: 2007 International Symposium on Computational Intelligence and Intelligent Informatics. IEEE, pp. 51–55. https://doi.org/10.1109/ISCIII.2007.367361.

Gonzalez, R.C., Woods, R.E.R.E., 2017. Digital Image Processing, fourth ed. Pearson.

Guzmán, E., Baeten, V., Pierna, J.A.F., García-Mesa, J.A., 2013. Infrared machine vision system for the automatic detection of olive fruit quality. Talanta 116, 894–898.

Hornberg, A., 2006. Handbook of Machine Vision. Wiley-VCH.

International Olive Council, 2000. World Catalogue of Olive Varieties. Technical Report, Madrid.

Justicia, M., Madueño, A., Ruiz-Canales, A., Molina, J., López, M., Madueño, J., Granados, J., 2017. Low-frequency characterisation of mesocarp electrical conductivity in different varieties of olives (*Olea europaea* L.). Comput. Electron. Agric. 142, 338–347.

Laaribi, I., Gouta, H., Ayachi, M.M., Labidi, F., Mars, M., 2017. Combination of morphological and molecular markers for the characterization of ancient native olive accessions in Central-Eastern Tunisia. Biologies 340, 287–297.

Likudis, Z., 2016. Olive oils with protected designation of origin (PDO) and protected geographical indication (PGI). In: Products from Olive Tree. InTech. https://doi.org/10.5772/64909.

Parra-López, C., Hinojosa-Rodríguez, A., Sayadi, S., Carmona-Torres, C., 2015. Protected designation of origin as a certified quality system in the Andalusian olive oil industry: adoption factors and management practices. Food Control 51, 321–332.

Pérez, N.F., Ferré, J., Boqué, R., 2009. Calculation of the reliability of classification in discriminant partial least-squares binary classification. Chemometr. Intell. Labor. Syst. 95, 122–128.

Piras, F., Grillo, O., Venora, G., Lovicu, G., Campus, M., Bacchetta, G., 2016. Effectiveness of a computer vision technique in the characterization of wild and farmed olives. Comput. Electron. Agric. 122, 86–93.

Ram, T., Wiesman, Z., Parmet, I., Edan, Y., 2010. Olive oil content prediction models based on image processing. Biosyst. Eng. 105, 221–232.

Russ, J.C., 2011. The Image Processing Handbook. CRC Press.

Sun, D.-W., 2016. Computer Vision Technology for Food Quality Evaluation. Elsevier/Academic Press.

Trujillo, I., Ojeda, M.A., Urdiroz, N.M., Potter, D., Barranco, D., Rallo, L., Diez, C.M., 2014a. Identification of the Worldwide Olive Germplasm Bank of Córdoba (Spain) using SSR and morphological markers. Tree Genet. Genomes 10, 141–155.

Trujillo, I., Ojeda, M.A., Urdiroz, N.M., Potter, D., Barranco, D., Rallo, L., Diez, C.M., 2014b. Identification of the Worldwide Olive Germplasm Bank of Córdoba (Spain) using SSR and morphological markers. Tree Genet. Genomes 10, 141–155.

Vanloot, P., Bertrand, D., Pinatel, C., Artaud, J., Dupuy, N., 2014. Artificial vision and chemometrics analyses of olive stones for varietal identification of five French cultivars. Comput. Electron. Agric. 102, 98–105.

Zhang, B., Huang, W., Li, J., Zhao, C., Fan, S., Wu, J., Liu, C., 2014. Principles, developments and applications of computer vision for external quality inspection of fruits and vegetables: a review. Food Res. Int. 62, 326–343.